

# Time-Resolved Sum-Frequency Generation Spectroscopy of Methoxy and Deuterated Methoxy on Ni(111) Using Near-Infrared Laser Pulses

Jun Kubota,<sup>\*,†</sup> Koji Kusafuka,<sup>†</sup> Akihide Wada,<sup>†</sup> Kazunari Domen,<sup>‡</sup> and Satoru S. Kano<sup>§</sup>

Chemical Resources Laboratory, Tokyo Institute of Technology, 4259 Nagatsuda, Midori-ku, Yokohama 226-8503, Japan, Department of Chemical System Engineering, The University of Tokyo, 7-3-1 Hongo, Bunkyo-ku, Tokyo 113-8656, Japan, and Faculty of Computer and Information Sciences, Hosei University, 3-7-2 Kajino-cho, Koganei, Tokyo 184-8584, Japan

Received: February 1, 2006; In Final Form: April 4, 2006

Methoxy (CH<sub>3</sub>O-) and deuterated (d-) methoxy (CD<sub>3</sub>O-) species on Ni(111) are investigated by sum-frequency generation (SFG) spectroscopy. Methoxy adsorbed on the Ni(111) surface is confirmed by SFG spectroscopy to be oriented normal to the surface. Two resonant peaks produced by methoxy, at 2921 and 2821 cm<sup>-1</sup>, are assigned to Fermi resonance between the CH symmetric stretching and overtone modes. Deuterated methoxy exhibits a single strong peak at 2051 cm<sup>-1</sup> assigned to the CD symmetric stretching mode. Investigation of the sub-nanosecond transient behavior of methoxy and d-methoxy species on Ni(111) under short-pulse laser pumping at 1064 nm reveals a clear weakening and recovery of the SFG peaks upon heating. The observed temporal profile is reproduced by simulation assuming that the original methoxy in the ground state is in chemical equilibrium with a new state produced by instantaneous heating. The dependence of the SFG spectra on the initial substrate temperature is also reproduced by the simulation. The simulation suggests a temperature jump of 250 K upon laser pumping, inducing a change in the molecular orientation or adsorption site of methoxy on the Ni(111) surface without decomposition of methoxy to adsorbed CO and hydrogen, which occurs under normal heating at 200 K.

## 1. Introduction

Pump-probe laser spectroscopy is widely employed for the investigation of surface dynamics.<sup>1,2</sup> The laser-driven temperature jump examined by this technique provides invaluable information on the behavior of short-lived excited species. Sum-frequency generation (SFG) spectroscopy, a pump-probe technique in which ultrashort laser pulses are used, has been successfully applied to the study of surface vibrational states.<sup>1–12</sup>

Exposure of metal and metal-oxide surfaces to nonresonant near-infrared (NIR) pump pulses results in thermal excitation at the surface, leading to surface chemical reactions<sup>5–9</sup> or thermal excitation of vibrational modes.<sup>10–12</sup> These phenomena are considered exotic, being driven by high yet extremely short-duration temperature jumps induced by laser irradiation. In the first 10 ps of irradiation, the temperatures of electrons ( $T_{\text{elec}}$ ), phonons ( $T_{\text{ph}}$ ), and adsorbates ( $T_{\text{ads}}$ ) diverge from equilibrium, and the resultant laser-induced chemical reactions, which differ from normal thermal reactions, can be studied with high temporal resolution.<sup>12</sup> Even for longer pulses of 30 ps or more, during which  $T_{\text{elec}}$ ,  $T_{\text{ph}}$ , and  $T_{\text{ads}}$  approach equilibrium, the transient jump in temperature can allow chemical reaction pathways that are normally kinetically suppressed to proceed.<sup>5,6,9</sup>

The vibrational excitation of surface molecules by laser pumping has been studied intensively.<sup>10–12</sup> The spectral changes induced by laser pumping include broadening and/or frequency shift of the vibrational bands, which originate from thermalized

low-frequency modes such as frustrated translation modes.<sup>11</sup> These spectral changes are typically much more pronounced than those that occur under normal heating, since the temperature jump is much higher than the regular desorption/decomposition temperature.<sup>11</sup> The excitation of vibrational modes has been studied extensively for CO/metal systems.<sup>10–12</sup> During the very short high-temperature period in laser pumping, desorption or decomposition of surface species is less likely to occur, allowing species to stay on the surface even at temperatures higher than those usually required for desorption/decomposition. Transient laser-induced changes in the structures of formates on NiO(111) have also been observed.<sup>6</sup> When exposed to NIR pump pulses, the formates on NiO(111) undergo structural change without decomposition, whereas decomposition readily occurs under normal heating.<sup>6</sup> CO molecules have similarly been observed to switch between on-top sites and hollow sites in the CO/Ni(111) system under NIR pulse pumping.<sup>5</sup> These structural changes are thought to represent elemental steps in the surface chemical reactions of thermally excited molecules.

Methanol appears in various heterogeneous catalytic and electrochemical reactions on surfaces,<sup>13,14</sup> undergoing molecular adsorption to surfaces at low temperatures and decomposing to form methoxy species on metal surfaces at higher temperatures. The vibrational spectra of methanol and methoxy on Ni(111) have been studied by infrared reflection absorption spectroscopy (IRAS)<sup>15</sup> and high-resolution electron energy loss spectroscopy (HREELS).<sup>16</sup> The assignment of vibrational bands, and thus molecular orientation, for methoxy has long been a subject of controversy.<sup>15–24</sup> However, a consensus seems to have been reached, and it is now generally accepted that methoxy stands vertically on flat surfaces, producing a symmetric CH stretching band accompanied by combination and/or overtone bands with

\* Corresponding author. Fax: +81-45-924-5282. E-mail: jkubota@res.titech.ac.jp.

<sup>†</sup> Tokyo Institute of Technology.

<sup>‡</sup> The University of Tokyo.

<sup>§</sup> Hosei University.

intensities gained by Fermi resonance.<sup>19–24</sup> This molecular orientation of methoxy has been confirmed by photoelectron diffraction.<sup>25–27</sup> Methoxy further decomposes to CO and hydrogen atoms on Ni(111) at around 200–250 K, and the CO and hydrogen thus desorb at 420 and 370 K, respectively. Although SFG spectra have been reported for methanol and methoxy species in the production of CO by methoxy decomposition on Ni(100),<sup>28</sup> time-resolved pump–probe SFG spectroscopy has yet to be performed for the methoxy species.

This paper describes the behavior of methoxy species on Ni(111) upon exposure to NIR pulses based on time-resolved SFG spectroscopy over a range of substrate temperatures. The change in the SFG signal due to NIR irradiation is found not to be attributable to the thermal broadening/weakening of the SFG peak but rather to changes in molecular structure. Prior to time-resolved experiments, the SFG spectral features of methoxy without pumping are assigned to confirm the molecular orientation of the species.

## 2. Experimental Section

Two different laser systems were employed for observation of the CH and CD stretching regions. For analysis of the CH stretching region, the system used was the same as that adopted in previous experiments.<sup>29,30</sup> Frequency-tunable IR pulses (2500–4000  $\text{cm}^{-1}$ ) were generated by an optical parametric oscillator/amplifier (OPO/OPA), in which LiNbO<sub>3</sub> crystals were used with the fundamental output of a Nd:YAG (1064 nm) laser (full-width at half-maximum of 35 ps, repetition rate of 10 Hz). The bandwidth of IR pulses was 5.3  $\text{cm}^{-1}$  (full-width at half-maximum) at 2600  $\text{cm}^{-1}$ . Visible pulses for SFG were obtained from the second harmonic output (532 nm) of the Nd:YAG laser. The energies of the IR and visible pulses at the sample surface were 150  $\mu\text{J}$  per pulse (at 2800  $\text{cm}^{-1}$ ) and 100  $\mu\text{J}$  per pulse, respectively, and both beams were p-polarized at the sample surface. For analysis of the CD stretching region, the laser system was optimized for observation in the 2000–2500  $\text{cm}^{-1}$  range.<sup>5,6,31,32</sup> To obtain frequency-tunable IR pulses in this frequency region, frequency-tunable NIR pulses were generated by an OPO/OPA system using  $\beta\text{-BaB}_2\text{O}_4$  (BBO) crystals from the second harmonic output (532 nm). Frequency-tunable mid-IR pulses (1300–3000  $\text{cm}^{-1}$ ) were then obtained from the tunable NIR pulses by differential frequency generation (DFG) using an AgGaS<sub>2</sub> (AGS) crystal with the fundamental output (1064 nm). The bandwidth of IR pulses was 4.7  $\text{cm}^{-1}$  (full-width at half-maximum) at 2000  $\text{cm}^{-1}$ . The energies of the IR (at 2000  $\text{cm}^{-1}$ ) and visible (at 532 nm) pulses at the sample surface were 50 and 100  $\mu\text{J}$  per pulse, respectively. Both beams were p-polarized at the sample surface.

For the pump–probe experiments, the sample was exposed to pump pulses (1064 nm) with an energy of 10 mJ per pulse. The timing of pulses was tuned using a variable optical delay device. The beam diameters of the IR, visible, and pump pulses were approximately 2, 3, and 5 mm, respectively. The SFG signal was detected using a photomultiplier tube after passage through optical filters and a monochromator.

The Ni(111) sample substrate was handled in an ultrahigh vacuum chamber pumped down to a base pressure of  $2 \times 10^{-8}$  Pa. The temperature of the sample (120–1000 K) was controlled by liquid nitrogen cooling and resistive heating. The sample surface was cleaned by repeated cycles of Ar<sup>+</sup> bombardment and annealing at 1000 K. The cleanness and long-range structure of the surface were monitored by Auger electron spectroscopy (AES) and low-energy electron diffraction (LEED), respectively, using a four-grid retarding field analyzer. Methanol and fully

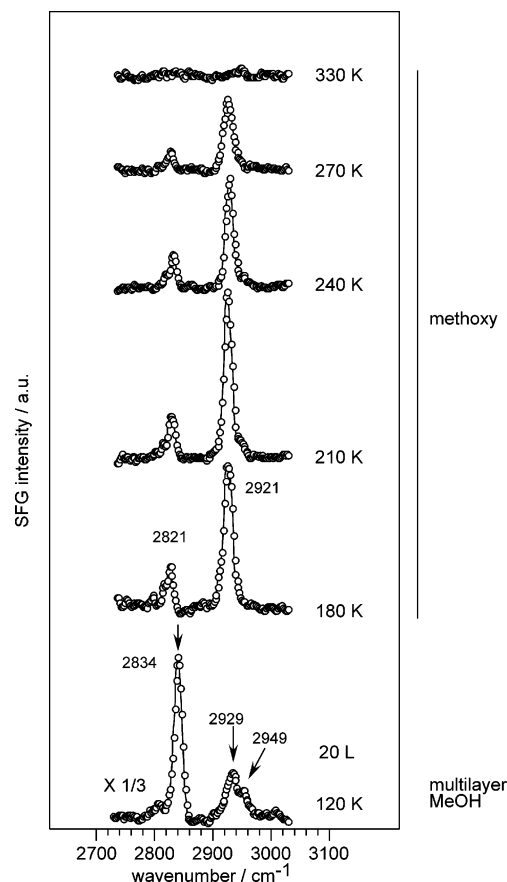


**Figure 1.** SFG spectra of methanol on Ni(111). The spectral resolution is 16  $\text{cm}^{-1}$ .

deuterated (d-) methanol ( $\text{CD}_3\text{OD}$ ) were dried using anhydrous copper sulfate and then purified by freeze–pump–thaw cycles prior to experiments.

In nonpumping experiments, 20 L of methanol or fully deuterated methanol was exposed to Ni(111) (1 L =  $1 \times 10^{-6}$  Torr·s, 1 Torr = 133 Pa) at 120 K and the sample was heated to 330 K. For the series of laser pumping experiments, the Ni(111) surface was first exposed to methanol gas and then annealed at 200 K. This procedure ensured that only methoxy could adsorb to the substrate with hydrogen atoms produced by the decomposition of methanol. Laser pumping measurements were then performed at substrate temperatures of 110–180 K. Because the experiment was carried out in a vacuum, the coverage of methoxy was kept constant and no decomposition of methoxy occurred throughout this experiment.

## 3. Results and Discussion

**3.1. SFG Spectra without Pumping.** (a) *SFG Spectra of Methoxy.* The SFG spectra of methoxy at various substrate temperatures without pumping are shown in Figure 1. Three peaks, at 2834, 2929, and 2949  $\text{cm}^{-1}$ , were observed at 120 K and assigned to the CH symmetric stretching ( $\nu_{\text{s(CH)}}$ ) mode, an overtone of the CH<sub>3</sub> symmetric deformation ( $2\delta_{\text{s(CH}_3\text{)}}$ ) mode and the CH asymmetric stretching ( $\nu_{\text{as(CH)}}$ ) mode of methanol molecules in the multilayer, respectively.<sup>22</sup> At 180 K, however, the peaks due to methanol in the multilayer disappeared to be replaced by new peaks at 2821 and 2921  $\text{cm}^{-1}$ . The 2821  $\text{cm}^{-1}$  peak was assigned to the symmetric CH stretching mode, and the 2921  $\text{cm}^{-1}$  peak, to the overtone mode on the basis of the frequency ratio of H/D as discussed later. The Fermi resonance between the CH symmetric stretching mode and the overtone

of the asymmetric  $\text{CH}_3$  deformation mode ( $2\delta_{\text{as}(\text{CH}_3)}$ ) causes the appearance of the latter mode in the SFG spectrum.<sup>19–21,23,24</sup> This assignment implies that the molecular axis of the methoxy stands vertical to the Ni(111) surface. These peaks were previously assigned to the symmetric and asymmetric CH stretching modes of methoxy species, the molecular axis of which was assumed to be tilted.<sup>15,16,28</sup> Subsequent discussions, however, have indicated that these peaks are assignable to the CH symmetric and overtone modes, having acquired significant intensity by Fermi resonance, suggesting that the methoxy species stand perpendicular to the surface.<sup>19–21,23,24</sup> This assignment is confirmed here by comparison with the SFG data for deuterated methoxy as presented later. The perpendicular orientation of methoxy on Ni(111) has also been suggested from observations of photoelectron diffraction, which reveals methoxy to be located at the 3-fold hollow site of Ni(111) with  $\text{C}_{3v}$  symmetry.<sup>27</sup>

The peaks were weaker at substrate temperatures greater than 210 K, and the methoxy peaks disappeared at 330 K. This can be attributed to the decomposition of methoxy to CO and hydrogen. Previously reported IRAS spectra also support this result.<sup>15</sup>

The vibrationally resonant peaks in the SFG spectra for methanol and methoxy on the Ni(100) surface have been reported to have dispersive shapes (asymmetric profiles) due to interference with the strong nonresonant background signal generated from the surface.<sup>28</sup> In the present SFG spectra, however, no appreciable modification of the peaks by background signal was observed. Note that a weak background signal allows for an uncomplicated, detailed signal analysis.

**(b) SFG Spectra of Deuterated Methoxy.** The spectra observed for the d-methanol system are shown in Figure 2. Three peaks, at 2071, 2127, and 2207  $\text{cm}^{-1}$ , were observed at 120 K for multilayered d-methanol and assigned to the symmetric CD stretching ( $\nu_{\text{s}(\text{CD})}$ ) mode, a combination of the CO stretching and  $\text{CD}_3$  symmetric deformation ( $\nu_{(\text{CO})} + \delta_{\text{s}(\text{CH}_3)}$ ) modes and the degenerate CD stretching ( $\nu_{\text{d}(\text{CD})}$ ) mode of d-methanol, respectively.<sup>19,23</sup> At temperatures above 150 K, however, a single strong peak appeared at 2051  $\text{cm}^{-1}$  and was assigned to the symmetric stretching mode ( $\nu_{\text{s}(\text{CD})}$ ) of d-methoxy. The CD asymmetric stretching band of d-methoxy is expected to appear between 2150 and 2250  $\text{cm}^{-1}$ , with the same temperature dependence as the symmetric stretching mode.<sup>19</sup> The previous assignment based on a tilted molecular axis, in which the molecular structure must be the same regardless of the isotopic speciation, suggests that there should be two similar peaks due to the CD symmetric and asymmetric modes in the d-methoxy spectra. It is thus evident that methoxy stands vertically on the surface, giving rise to a single CD symmetric band.

In the spectra for d-methoxy, a small peak was also observed at 2160  $\text{cm}^{-1}$ , having a temperature dependence different from that for the 2051  $\text{cm}^{-1}$  peak. This weak peak may originate from d-methoxy at defect sites, as suggested by the persistence of this small peak to higher temperatures than the 2051  $\text{cm}^{-1}$  peak. The frequency of this small peak corresponds to the overtone of the  $\text{CD}_3$  symmetric deformation mode ( $2\delta_{\text{s}(\text{CD}_3)}$ ).<sup>19,23</sup> This species seems to be an impurity, and a detailed discussion is avoided.

At a surface temperature of 320 K, a new peak appeared at 2026  $\text{cm}^{-1}$ . This peak is clearly due to on-top CO molecules formed by the decomposition of methoxy species.<sup>33,34</sup> CO on Ni(111) can occupy both the bridged and on-top sites, with most CO molecules locating on bridged sites after the decomposition of methoxy at 320 K. The vibrational peak of the bridged CO

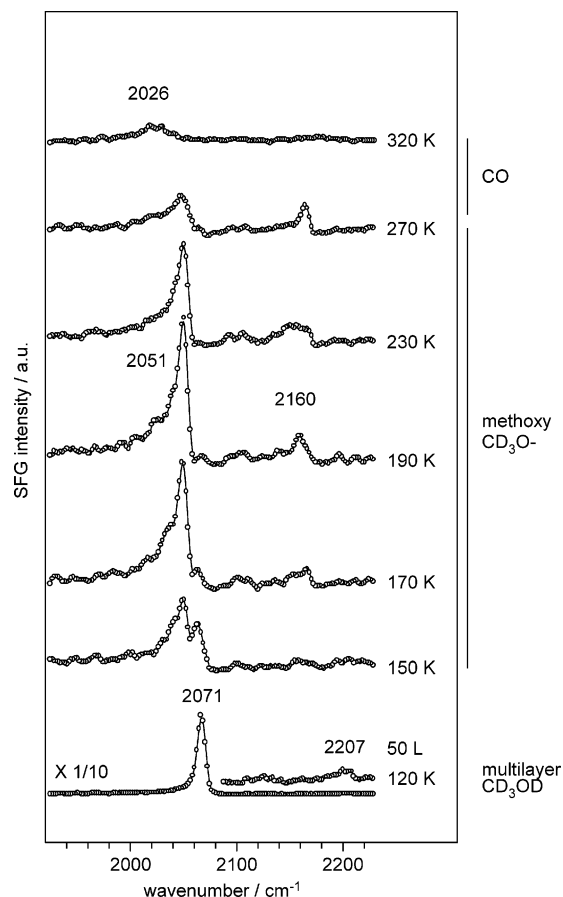


**Figure 2.** SFG spectra of d-methanol on Ni(111). The spectral resolution is 4  $\text{cm}^{-1}$ .

molecules is expected to be observed at around 1830  $\text{cm}^{-1}$ .<sup>33,34</sup> The SFG counterpart, however, is too weak to detect.<sup>34</sup>

**(c) Remarks.** The H/D frequency ratios for the 2051  $\text{cm}^{-1}$  peak are 1.375 with respect to the 2821  $\text{cm}^{-1}$  peak and 1.424 with respect to the 2921  $\text{cm}^{-1}$  peak. This confirms that the peak at 2821  $\text{cm}^{-1}$  for methoxy is mainly due to CH symmetric vibrations, for which the H/D frequency ratio is usually less than  $\sqrt{2}$ .<sup>19–24</sup> The peak at 2921  $\text{cm}^{-1}$  for methoxy is thus confirmed to be due to a combination mode with intensity produced by Fermi resonance.

There is no clear explanation for the substantial strength of the 2921  $\text{cm}^{-1}$  peak. Peaks augmented by Fermi resonance are still generally weaker than the fundamental mode. However, the 2921  $\text{cm}^{-1}$  peak is stronger than the 2821  $\text{cm}^{-1}$  peak, even in IRAS measurements,<sup>16</sup> and this feature certainly does not originate from nonlinear processes or coherent artifacts of SFG spectroscopy. This feature of Fermi resonance appears to be specific to Ni(111) surfaces. In the case of methoxy on Cu(111) and Cu(100), for example, the combination bands at 2875–2918  $\text{cm}^{-1}$  are weaker than the CH symmetric stretching band.

### 3.2. Transient SFG Signals under Laser Pulse Pumping.

**(a) Dynamic Behavior of Methoxy.** The NIR pump pulse was not resonant with any electronic transitions of the adsorbed species, and the observed recovery time was much longer than the characteristic time of electronic de-excitation at metal surfaces.<sup>10–12</sup> The transient behavior of the SFG signals is thus confidently attributed to thermal excitation of the surface.

Transient changes in the spectra at 130 and 180 K are shown in Figure 3. These spectra were obtained at fixed delay times of 150 ps before and 50 and 150 ps after the pump pulse. The

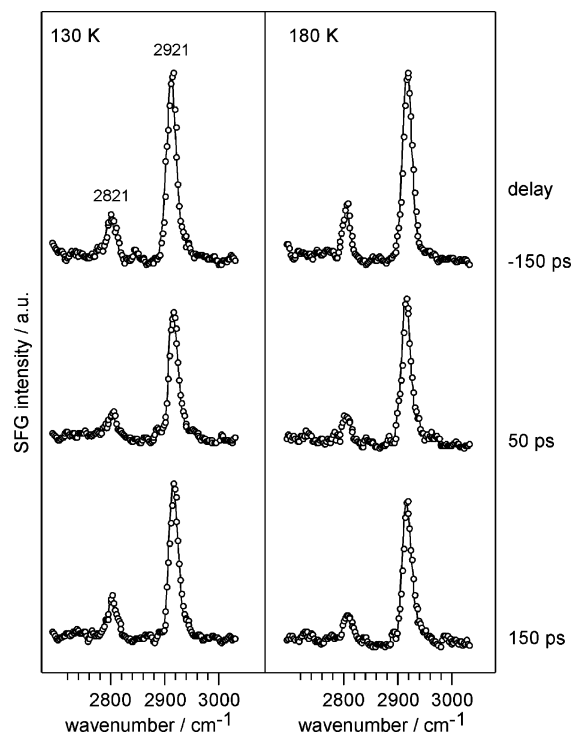


**Figure 3.** Transient SFG spectra of methoxy on Ni(111) at 130 and 180 K.

signal intensities of the 2821 and 2921  $\text{cm}^{-1}$  peaks decreased by 25% due to pumping, regardless of the initial temperature. As significant broadening of the SFG peaks due to pumping was not observed, the signal weakening was considered to represent a decrease in the number density of species. From the quadratic nature of SFG intensity,<sup>1–4</sup> this result suggests

that  $\sqrt{1-0.25} \approx 87\%$  of the original species remained unchanged. Therefore, if this decrease corresponds to a decrease in the number of relevant species, 13% of the species appear to have been transformed to a new state. New resonant peaks may thus appear, but the SFG intensities of the new peaks are likely to be too low to be observed. One important point as seen in Figure 3 is that no spectral broadening was observed by pumping and temperature difference between 130 and 180 K. The width of the 2921  $\text{cm}^{-1}$  band at full-width at half-maximum was ca. 20  $\text{cm}^{-1}$  even before and after pumping at 130 and 180 K.

Another important feature of the transient spectra is the speed of signal intensity recovery at 130 K, which appears to be faster than at 180 K. This trend is obvious from the transient changes in signal intensities at 2921  $\text{cm}^{-1}$  (Figure 4a) and 2821  $\text{cm}^{-1}$  (Figure 4b) for methoxy at 110–170 K. The intensities were suppressed by pulse irradiation but then recovered within several hundreds picoseconds. This recovery time increased with increasing temperature. Above 170 K, a considerable fraction of the methoxy underwent decomposition and the transient intensity change could not be examined.

(b) *Dynamic Behavior of Deuterated Methoxy.* The transient behavior of d-methoxy indicated by the SFG spectra was largely identical to that for methoxy. Figure 5 shows the spectral change due to NIR pumping and the transient variation in the peak due to the CD symmetric stretching mode at 2051  $\text{cm}^{-1}$ . Note that no new peaks appeared due to pumping, as in the case of methoxy.

The two slight differences observed between the methoxy and d-methoxy spectra are a lower peak intensity (35% lower) and slightly faster recovery of the 2051  $\text{cm}^{-1}$  SFG signal for d-methoxy. No clear reasons for these differences can be suggested at present, and they may be attributable to isotope effects or a difference of experimental conditions.

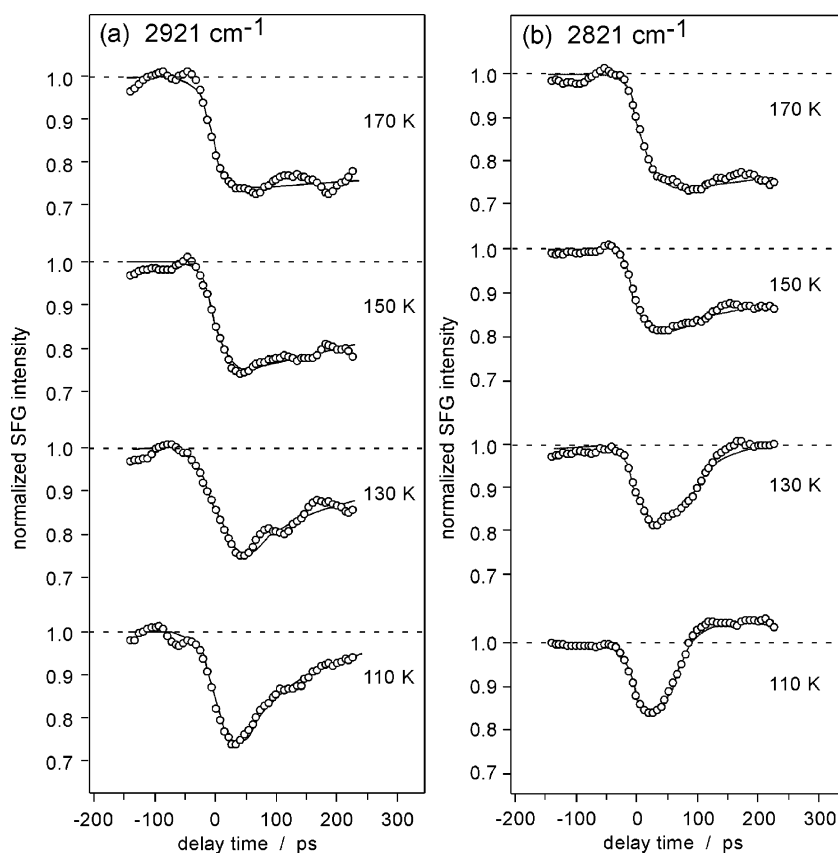


**Figure 4.** Temporal profiles of the SFG signal at (a) 2921  $\text{cm}^{-1}$  and (b) 2821  $\text{cm}^{-1}$  for adsorption of methoxy on Ni(111) at various temperatures.



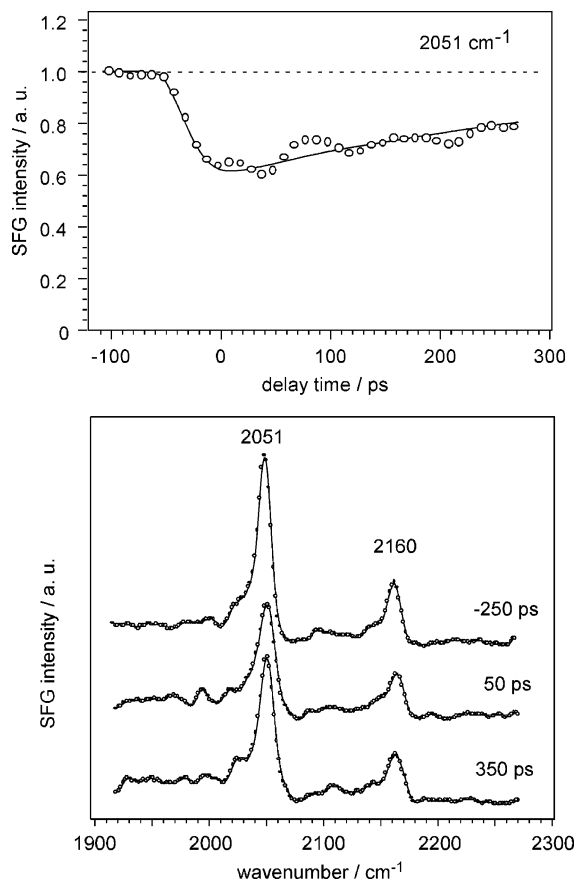


**Figure 5.** Temporal profiles of the SFG signal at 2051 cm<sup>-1</sup> and transient SFG spectra of d-methoxy adsorbed on Ni(111) at 190 K.

Summarizing the results of time-resolved measurements on methoxy and d-methoxy, the amount of decrease of the SFG signal intensity by the pumping was ca. 25% between 110 and 170 K, regardless of the substrate initial temperature. The recovery time increased with increasing the temperature. Neither methoxy nor d-methoxy showed a new peak corresponding to the new species by the irradiation.

**3.3. Model of Structural Transition.** (a) *Vibrational Relaxation and Chemical Reaction.* As no temperature dependence of line broadening was observed, some other process must be responsible for the transient weakening of the SFG signal upon laser pumping. It may be appropriate, however, to briefly discuss the temperature-dependent part of the line broadening. When low-frequency modes of adsorbed species are thermally excited, vibrational bands coupled with low-frequency modes become broader, accompanied by a decrease in the corresponding peak intensity of IR absorption.<sup>11,12</sup> As the intensity decreases almost linearly (monotonically) with increasing temperature,<sup>35,36</sup> the temporal profile of intensity reflects the profile of surface temperature. Simulations suggest that the temporal profile of surface temperature after pumping is not critically dependent on the initial temperature. Thus, thermal broadening of the band cannot be expected in the present case to be responsible for the observed transient change in the SFG spectra, which exhibit a dependence on the initial temperature. The peak intensity in SFG is in inverse proportion to the square of the bandwidth,<sup>1,2</sup> so that it is strongly affected by the bandwidth. While band broadening was not observed as described in the previous section, one possibility still remains that the band broadening by the pumping occurred within the experimental resolution (5.3 cm<sup>-1</sup>) and affected the signal weakening. Thus, simulation to

**TABLE 1: Parameters Used for the Simulation**

parameter	notation	value	note
heat diffusibility	$\kappa$	$2.3 \times 10^{-5} \text{ m}^2 \cdot \text{s}^{-1}$	<i>a</i>
heat capacity per volume	$C$	$4.0 \times 10^6 \text{ J} \cdot \text{m}^{-3} \cdot \text{K}^{-1}$	<i>b</i>
absorption coefficient	$\alpha$	$0.060 \text{ nm}^{-1}$	<i>c</i>
pulse width	$\tau$	21 ps	<i>d</i>

<sup>a</sup> Heat diffusibility  $\kappa = \lambda/C$  ( $\lambda$  thermal conductivity in  $\text{W} \cdot \text{m}^{-1} \cdot \text{K}^{-1}$ ).<sup>41</sup>  
<sup>b</sup>  $C = C_p \rho$  ( $C_p$  specific heat capacitance in  $\text{J} \cdot \text{kg}^{-1} \cdot \text{K}^{-1}$ ,  $\rho$  density in  $\text{kg} \cdot \text{m}^{-3}$ ).<sup>41</sup> <sup>c</sup>  $4\pi k/\lambda$  ( $k$  imaginary component of refractive indices,  $\lambda$  wavelength 1064 nm).<sup>41</sup> <sup>d</sup> The term  $\tau_{\text{fwhm}}/2\sqrt{\ln 2}$  ( $\tau_{\text{fwhm}}$  pulse width as fwhm 35 ps).

clarify the relation among the temperature, delay time, and SFG intensity during pumping was carried out in the following subsection.

The rates of vibrational relaxation and chemical reaction, however, are dependent on temperature. These rate constants generally increase with temperature, as observed in many experiments. In pump-probe analysis of surface species, vibrational relaxation of the symmetric mode of CH<sub>3</sub> in methylthiolate (CH<sub>3</sub>S-) on Ag(111) is a typical example.<sup>37</sup> The vibrational relaxation of molecules adsorbed on metal surfaces is generally faster than the present pulse duration time because of electron-hole pair damping.<sup>38,39</sup> The recovery time observed in the present experiments, which increases with increasing temperature, clearly does not vary in accordance with this phenomenon.

(b) *Simulation of Surface Temperature and SFG Signal Intensity.* A simulation of surface temperature change due to laser pumping was conducted using a one-dimensional heat diffusion equation,<sup>40</sup> as given by

$$\frac{\partial T(z,t)}{\partial t} = \kappa \frac{\partial^2 T(z,t)}{\partial z^2} + \frac{I\alpha}{C} \exp(-\alpha z) \exp\left(\frac{-t^2}{\tau^2}\right) \quad (1)$$

where  $T(z,t)$  is the temperature at depth  $z$  and time  $t$ ,  $\kappa$  is the heat diffusibility of Ni (i.e., thermal conductivity per heat capacity),  $I$  is the absorbed pulse power per unit area,  $C$  is the heat capacity of Ni per unit volume,  $\alpha$  is the absorption coefficient for Ni per unit length, and  $\tau$  is the pulse width. The values of physical parameters employed in the simulation are listed in Table 1.<sup>41</sup> Vibrational relaxation of adsorbed molecules on metal surfaces is generally faster than several picoseconds due to the presence of electron-hole pair damping into the metal substrate.<sup>39</sup> It is assumed that the system of electrons, phonons, and adsorbed species achieves equilibrium within  $\tau$ , and a single temperature  $T$  is used throughout in the present pulse duration.

To convert the information of  $T$  into an SFG signal intensity, the following assumption is introduced. Assuming the total number density of methoxy remains constant, a decrease in SFG signal intensity represents conversion of methoxy into other surface structure(s) that cannot be observed by SFG. The ratio of the original form of methoxy to alternative forms is determined on the basis of chemical equilibrium and is thus a function of temperature. This can be described by

$$P(T(0,t)) = P_0 \theta(T(0,t))^2 \quad (2)$$

and

$$\frac{1 - \theta(T(0,t))}{\theta(T(0,t))} = \exp\left(\frac{\Delta S}{R}\right) \exp\left(\frac{-\Delta H}{RT(0,t)}\right) \quad (3)$$

where  $P(T(0,t))$  is the SFG intensity at surface temperature  $T$  and original methoxy coverage  $\theta$ , and  $P_0$  is the initial SFG

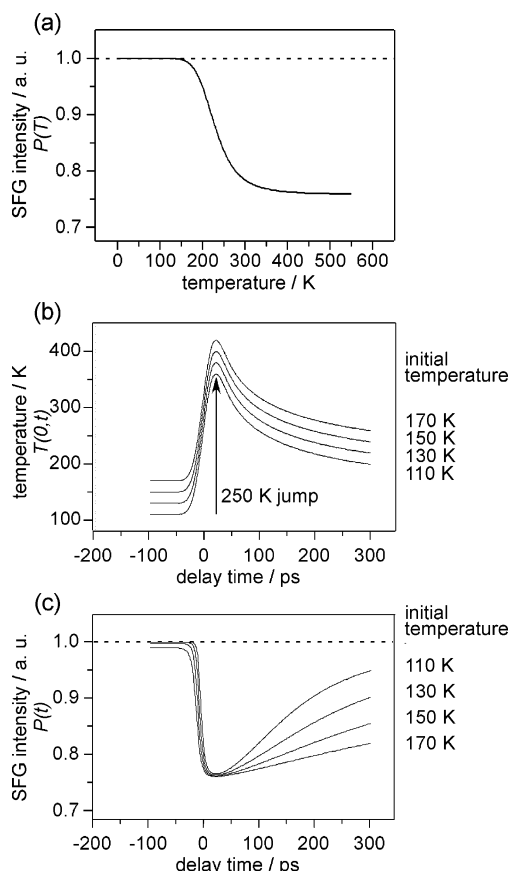


**Figure 6.** Simulation of transient behavior of the SFG signal for methoxy adsorption on Ni(111). (a) Variation in SFG intensity with respect to temperature. (b) Temperature jump at the surface with respect to time following laser pumping. (c) Measured SFG intensity response corresponding to b.

intensity. Equation 2 indicates that the SFG intensity is proportional to the square of the molecular density. The parameters  $\Delta H$  and  $\Delta S$  in eq 3 are the enthalpy and entropy factors of equilibrium, and  $R$  is the gas constant. The surface temperature  $T(0,t)$  is derived from eq 1. Equation 3 indicates that some fraction of the methoxy species is converted to another species (not observable by SFG) and that the new species are in equilibrium with the original form of methoxy.

The parameters  $I$ ,  $\Delta S$ , and  $\Delta H$  are fitted to the data so as to achieve the observed temporal SFG response. The calculated profiles  $P(T)$ ,  $T(0,t)$ , and  $P(t)$  are shown in Figure 6. The best fit was obtained with  $\Delta S$  and  $\Delta H$  values of  $0.074 \text{ kJ}\cdot\text{K}^{-1}\cdot\text{mol}^{-1}$  and  $17 \text{ kJ}\cdot\text{mol}^{-1}$ , with a temperature jump of 250 K from the initial temperature (see Figure 6c). This temperature jump of 250 K is almost the same as that estimated previously for the formate/NiO system.<sup>6,31</sup> The observed features of the temperature dependence of the time-resolved SFG were reproduced satisfactorily: the signal decrease by 25% at all temperatures, and the recovery times increase with increasing initial temperature.

(c) *Proposed Model of Transient Structural Change under Laser Pumping.* A key feature of the proposed model is the temperature dependence of SFG signal intensity (Figure 6a), which is vastly different from that due to thermal broadening or thermal shift (i.e., monotonic increase with temperature).<sup>35,36</sup> The thermal broadening, thermal shift, and corresponding signal weakening caused by the temperature jump originate from the coupling of the fundamental C–H (C–D) stretching modes with the low-frequency modes such as frustrated modes. The vibrational distributions in the low-frequency modes cannot

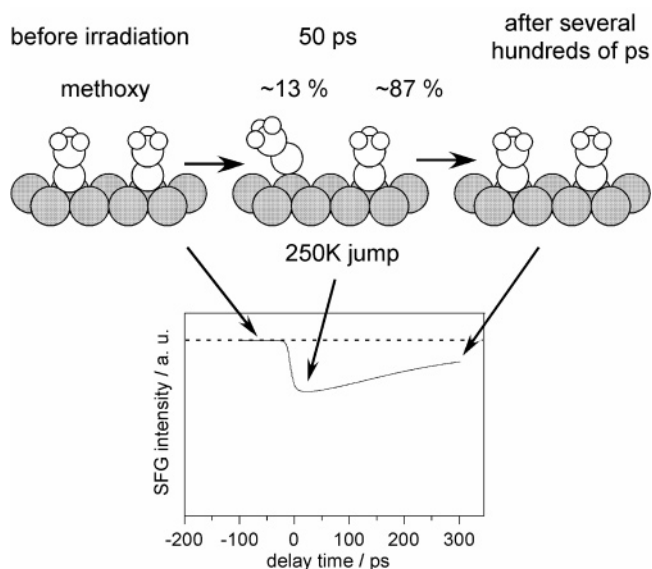


**Figure 7.** Proposed transient behavior of methoxy upon irradiation with short laser pulses.

saturate by temperature, and the behavior of signal weakening by heating should be similar to that for CO/metal systems.<sup>35,36</sup> Thus, the signal weakening shown in Figure 6a, which is almost constant above 400 K, cannot be attributed from the vibrational distributions of the low-frequency modes. Note that  $P(T)$  (Figure 6a) changes dramatically at around 200 K. In the case of normal heating, methoxy starts to decompose at this temperature.<sup>15,16</sup> This suggests that methoxy changes to a new state at 200 K prior to decomposition. In the case of laser pumping using very short pulses, this change is transient and recovers after a few hundred picoseconds without decomposition.

The new state is presumably tilted methoxy and/or methoxy located at alternative surface sites. The 25% decrease in signal intensity suggests that 13% of the methoxy population is converted to a new state. However, even if all of the new methoxy contributes to a new band with the same SFG susceptibility as the original methoxy form, the intensity of the new band will be less than 2% of that of the original SFG peak ( $0.13^2$ ) and thus virtually undetectable by SFG spectroscopy. If the new form is tilted methoxy, the new band corresponding to the CH asymmetric mode may indeed be active in SFG, similar to its symmetric counterpart.

Methoxy is stable below 200 K in the present experiments, indicating that the activation barrier for decomposition of methoxy is ca.  $60 \text{ kJ}\cdot\text{mol}^{-1}$ .<sup>42–44</sup> It is unrealistic to assume that the methoxy changes transiently to formyl (CHO-) or other chemical species and then returns back to methoxy after irradiation. Note that the obtained value of  $\Delta H$ ,  $17 \text{ kJ}\cdot\text{mol}^{-1}$ , suggests that the potential barrier to the new species is not particularly high.

It is usually assumed that the migration of surface species begins at the decomposition temperature. When migrating methoxy species occupy unstable surface sites, the structure may change, giving rise to a decrease in the SFG intensity of the original band (Figure 7). In the transient SFG spectra, however, no new peaks assignable to new species could be observed upon pumping. Detailed discussion on the new structures or sites remains a topic of future research.

#### 4. Conclusion

The initial structure of methoxy on the Ni(111) surface was determined by comparing the vibrational spectra with that of

d-methoxy without pumping. The methoxy produced two SFG peaks, at 2921 and 2821  $\text{cm}^{-1}$ , in the C–H stretching region, assigned to the CH symmetric stretching and combination modes, respectively. For d-methoxy, the strong peak observed at 2051  $\text{cm}^{-1}$  was assigned to the CD symmetric stretching mode. These assignments are consistent with the notion that methoxy is oriented perpendicular to the surface.

Transient features in the SFG spectra of the C–H stretching mode of methoxy on Ni(111) were examined as a function of the initial substrate temperature. The vibrational resonant SFG intensities weakened transiently after irradiation yet recovered on a subnanosecond time scale. The time-dependent variation in SFG intensity was successfully simulated assuming that chemical equilibrium between the ground state and excited methoxy is achieved with relatively low enthalpy. The simulation thus suggests the transformation of methoxy species to a new structure by short-pulse irradiation. The SFG signal of methoxy steps down at 200 K, corresponding to the decomposition temperature under normal heating. The temperature jump is estimated to be 250 K, and the species return to the original state within a sub-nanosecond time frame as the temperature returns to baseline. Decomposition does not occur even above 200 K in the case of short-pulsed heating. These features can be attributed to change of the original methoxy into new species with low SFG susceptibility that migrate among surface sites. Thermal broadening/weakening of the vibrational band is unable to explain these observations.

## References and Notes

- (1) *Laser spectroscopy and photochemistry on metal surfaces part I and II*; Dai, H.-L., Ho, W., Eds.; World Scientific: Singapore, 1995.
- (2) Rubahn, H.-G. *Laser applications in surface science and technology*; John Wiley & Sons: New York, 1999.
- (3) Rupprechter, G. *Phys. Chem. Chem. Phys.* **2001**, *3*, 4621.
- (4) Buck, M.; Himmelhaus, M. *J. Vac. Sci. Technol. A* **2001**, *19*, 2717.
- (5) Kubota, J.; Yoda, E.; Ishizawa, N.; Wada, A.; Domen, K.; Kano, S. S. *J. Phys. Chem. B* **2003**, *107*, 10329.
- (6) Bandara, A.; Kubota, J.; Onda, K.; Wada, A.; Kano, S. S.; Domen, K.; Hirose, C. *J. Phys. Chem. B* **1998**, *102*, 5951.
- (7) Bonn, M.; Kleyn, A. W.; Kroes, G. J. *Surf. Sci.* **2002**, *500*, 475.
- (8) Bonn, M.; Funk, S.; Hess, Ch.; Denzler, D. N.; Stampfl, C.; Schffler, M.; Wolf, M.; Ertl, G. *Science* **1999**, *285*, 1042.
- (9) Schröder, U.; Guyot-Sionnest, P. *Surf. Sci.* **1999**, *421*, 53.
- (10) Hess, Ch.; Wolf, M.; Roke, S.; Bonn, M. *Surf. Sci.* **2002**, *502–503*, 304.
- (11) Bonn, M.; Hess, Ch.; Funk, S.; Miners, J. H.; Wolf, M.; Ertl, G. *Phys. Rev. Lett.* **2000**, *84*, 4653.
- (12) Germer, T. A.; Stephenson, J. C.; Heilweil, E. J.; Cavanagh, R. R. *J. Chem. Phys.* **1994**, *101*, 1704.
- (13) Masel, R. I. *Principles of adsorption and reaction on solid surface*; John Wiley & Sons: New York, 1996.
- (14) Somorjai, G. A. *Introduction to surface chemistry and catalysis*; John Wiley & Sons: New York, 1994.
- (15) Zenobi, R.; Xu, J.; Yates, J. T., Jr.; Persson, B. N. J.; Volokitin, A. I. *Chem. Phys. Lett.* **1993**, *208*, 414.
- (16) Demuth, J. E.; Ibach, H. *Chem. Phys. Lett.* **1979**, *60*, 395.
- (17) Ryberg, R. *Phys. Rev. B* **1985**, *31*, 2545.
- (18) Sexton, B. A. *Surf. Sci.* **1979**, *88*, 299.
- (19) Chesters, M. A.; McCash, E. M. *Spectrochem. Acta* **1987**, *43A*, 1625.
- (20) Dastoor, H. E.; Gardner, P.; King, D. A. *Chem. Phys. Lett.* **1993**, *209*, 493.
- (21) Weldon, M. K.; Uvdal, P.; Friend, C. M.; Serafin, J. G. *J. Chem. Phys.* **1995**, *103*, 5075.
- (22) Camplin, J. P.; McCash, E. M. *Surf. Sci.* **1996**, *360*, 229.
- (23) Huberty, J. S.; Madix, R. J. *Surf. Sci.* **1996**, *360*, 144.
- (24) Mudalige, K.; Warren, S.; Trenary, M. *J. Phys. Chem. B* **2000**, *104*, 2448.
- (25) Linder, Th.; Somers, J.; Bradshaw, A. M.; Kilcoyne, A. L. D.; Woodruff, D. P. *Surf. Sci.* **1988**, *203*, 333.
- (26) Hofmann, Ph.; Schindler, K.-M.; Bao, S.; Fritzsche, V.; Ricken, D. E.; Bradshaw, A. M.; Woodruff, D. P. *Surf. Sci.* **1994**, *304*, 74.
- (27) Bradshaw, A. M.; Schaff, O.; Hess, G.; Fritzsche, V.; Fernandez, V.; Schindler, K.-M.; Hofmann, Ph.; Theobald, A.; Davis, R.; Woodruff, D. P. *Surf. Sci.* **1995**, *331–333*, 201.
- (28) Miragliotta, J.; Polizzotti, R. S.; Rabinowitz, P.; Cameron, S. D.; Hall, R. B. *Chem. Phys.* **1990**, *143*, 123.
- (29) Yuzawa, T.; Kubota, J.; Onda, K.; Wada, A.; Domen, K.; Hirose, C. *J. Mol. Struct.* **1997**, *413–414*, 307.
- (30) Yuzawa, T.; Shioda, T.; Kubota, J.; Onda, K.; Wada, A.; Domen, K.; Hirose, C. *Surf. Sci.* **1998**, *416*, L1090.
- (31) Hirose, C.; Bandara, A.; Katano, S.; Kubota, J.; Wada, A.; Domen, K. *Appl. Phys. B* **1999**, *68*, 559.
- (32) Kubota, J.; Wada, A.; Domen, K.; Kano, S. S. *Chem. Phys. Lett.* **2002**, *362*, 476.
- (33) Trenary, M.; Uram, K. J.; Bazso, F.; Yates, J. T., Jr. *Surf. Sci.* **1984**, *146*, 269.
- (34) Bandara, A.; Katano, S.; Kubota, J.; Onda, K.; Wada, A.; Domen, K.; Hirose, C. *Chem. Phys. Lett.* **1998**, *290*, 261.
- (35) Jakob, P.; Persson, B. N. J. *Phys. Rev. B* **1997**, *56*, 10644.
- (36) Persson, B. N. J.; Hoffmann, F. M.; Ryberg, R. *Phys. Rev. B* **1989**, *34*, 2266.
- (37) Harris, A. L.; Rothberg, L.; Dhar, L.; Levinos, N. J.; Dubois, L. H. *J. Chem. Phys.* **1991**, *94*, 2438.
- (38) Beckerle, J. D.; Casassa, M. P.; Cavanagh, R. R.; Heilweil, E. J.; Stephenson, J. C. *Phys. Rev. Lett.* **1990**, *64*, 2090.
- (39) Morin, M.; Levinos, N. J.; Harris, A. L. *J. Chem. Phys.* **1992**, *96*, 3950.
- (40) Bechtel, J. H. *J. Appl. Phys.* **1975**, *46*, 1585.
- (41) *CRC Handbook of chemistry and Physics*; Lide, D. R., Ed.; CRC Press: Boca Raton, FL, 1994.
- (42) Villarrubia, J. S.; Ho, W. *Surf. Sci.* **1984**, *144*, 370.
- (43) Richer, L. J.; Ho, W. *J. Chem. Phys.* **1985**, *83*, 2569.
- (44) Yasumori, I.; Nakamura, T.; Miyazaki, E. *Bull. Chem. Soc. Jpn.* **1967**, *40*, 1372.